Commensurability oscillations in the antidot lattice in a quasi-three-dimensional electron gas

N. M. Sotomayor, G. M. Gusev, and J. R. Leite

Instituto de Física da Universidade de São Paulo, Caixa Postal 66318, CEP 05315-970, São Paulo, Brazil

A. A. Bykov, L. V. Litvin, N. T. Moshegov, and A. I. Toropov

Institute of Semiconductor Physics, Novosibirsk, Russia

O. Estibals and J. C. Portal*

GHMFL, MPI-FKF/CNRS, Boite Postale 166, F-38042, Grenoble, Cedex 9, France

A three-dimensional electron billiard system is obtained by patterning a rectangular array of cylindrical voids in GaAs/Al$_x$Ga$_{1-x}$As parabolic quantum wells containing a high mobility quasi-three-dimensional electron gas. Resistivity (R_{xx}) measurements reveal anomalous broadened peaks in the low-field magnetoresistance, in a similar way as measurements in two-dimensional antidot systems. R_{xx} in a tilted magnetic field show that commensurability peaks transform continuously to different kinds of peaks that we attribute to geometrical resonances between the cyclotron radius (R_c) and the well width (W).

Up to date, most of the experimental and theoretical works, referring to electron billiards in semiconductor heterostructures, have been done in two-dimensional systems.[1,2] However, very few works concerning three-dimensional electron billiards have been done, especially, in the experimental research. On the other part, some numerical results on the stability of classical trajectories in fully chaotic and ergodic three-dimensional billiard systems have been recently published.[3,4] The three-dimensional electron gas (3DEG)[5] is another interesting physical system that can also be used to study the manifestations of quantum chaos in condensed matter physics. Recently its experimental realization has been accomplished in the so-called parabolic quantum wells (PQW).[6] These systems contain a wide layer of uniform, low-diluted, and highly mobile carriers, with strong electron-electron interaction. The introduction of an artificial array of cylindrical voids in a PQW sample approaches a three-dimensional electron billiard system and can be regarded as a natural extension of the study of the chaotic electron dynamics in condensed matter physics. This construction can be used to study the transition between the two-dimensional and three-dimensional chaotic electron dynamics, as well as the influence of the electron-electron interaction. In this Brief Report we report the fabrication and characterization of rectangular arrays of cylindrical antidots in parabolic quantum wells with well width $W = 2000$ Å, and different lattice period a. As in the case of antidots, in two-dimensional systems, a mixed electron dynamics is observed. We perform low-temperature magnetotransport measurements and found that, at low field, the resistivity R_{xx} is enhanced and commensurability oscillations appear. Two rather broad peaks are distinguished and the most prominent one corresponds to the commensurability condition $R_c = a/2$, where R_c is the cyclotron radius. Longitudinal resistivity measurements, in a tilted magnetic field, demonstrate that these oscillations do not shift continuously towards the higher values of the field as in the case of antidot lattices in two-dimensional systems.

A type of three-dimensional electron billiard system can be obtained by patterning a rectangular array of cylindrical voids in the Al$_x$Ga$_{1-x}$As/GaAs PQW. A cylindrical void is a convex dispersive boundary center where close electron orbits begin to diverge exponentially after first few collisions. As in the case of two-dimensional antidots, in the presence of perpendicular magnetic field, the coexistence of regular and chaotic orbits may be expected. If we define z as the direction perpendicular to the plane of the sample surface, electrons are confined by the parabolic potential along this direction and are free to move along the x-y plane. Figure 1(a) shows a schematic view of a multilayered semiconductor structure containing a PQW, with an imposed array of artificial cylindrical scatterers. d represents the lithographic antidot diameter, a the artificial lattice period, and W the width of the layer corresponding to the well. Figure 1(b) represents the three-dimensional real space region of the sample where the electrons are free to move. This region is limited by the interfaces corresponding to the barriers of the PQW and the cylindrical voids, which generate an array of potential pillars. The antidot samples were fabricated from a high-mobility GaAs/Al$_x$Ga$_{1-x}$As PQW, grown by molecular beam epitaxy with the next configuration: over a (100) semi-insulating GaAs substrate was deposited a 1.0-μm GaAs buffer layer, followed by 20 AlAs$_5$GaAs$_{10}$ periods (where 5 and 10 stand for the number of monolayers of each material). Over this superlattice was grown an undoped 8000 Å GaAs layer followed by 500 Å of Al$_x$Ga$_{1-x}$As with x varying from 0.07 to 0.27. Then follows, a 1000-Å Al$_{0.3}$Ga$_{0.7}$As layer, a Si-delta layer, a 100-Å undoped Al$_{0.3}$Ga$_{0.7}$As spacer, and the 2000-Å parabolic well with composition variation $0 < x < 0.19$. After the well come again a 100-Å undoped Al$_{0.3}$Ga$_{0.7}$As spacer, the Si-delta layer, and a 400-Å Al$_{0.3}$Ga$_{0.7}$As layer. Finally a 100-Å GaAs cap was deposited on the surface. After growing, a 50-μm-wide Hall bar was patterned for each sample by means of conventional techniques, a rectangular array (100×50 μm) of cylindrical-shaped artificial scatterers were superimposed over the
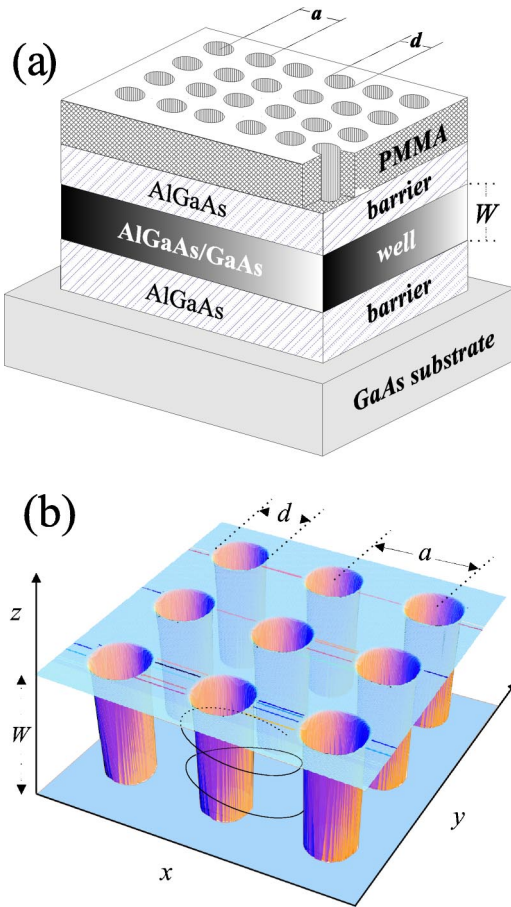
FIG. 1. (a) Scheme of a GaAs/Al$_x$Ga$_{1-x}$As heterostructure containing a lattice of cylindrical voids, transferred across the well and the barrier layers. (b) Real space region, corresponding to the well-electron slab, where the electron dynamics develops.

TABLE I. Commensurability peak position in perpendicular magnetic field, electron concentration, electron mobility, mean-free-path, and three-dimensional Fermi energy for each sample periodicity.

$a(\mu$m)	0.6	0.7	0.8
$peak1(T)$	0.18	0.15	0.15
$peak2(R_c/a)$	1.8	1.9	2.4
$n^+(*10^{16}$ cm$^{-3})$	2.2	2.3	2.5
$\mu_e(*10^4$ cm^2/V s)	5.8	4.3	5.0
E_F(meV)	4.3	4.4	4.7
$l(\mu$m)	0.3	0.2	0.3

electron mean-free-path l, varies between 0.2 and 0.3 μm. According to these data the electron transport in our samples can be treated in the quasiballistic regime $W<l<L$, where L is the channel length of the Hall bar. Table I summarizes the transport data for each of our samples. When submitted to a perpendicular magnetic field, the resistivity from the patterned region of the samples shows an enhancement at a low field, which is accompanied by two rather broad peaks and a negative magnetoresistance. Figure 2(a) shows the longitudinal resistivity R_{xx} at 1.4 K from the two regions of the sample with periodicity $a=0.8$ μm.

The two commensurability peaks are located at the positions corresponding to $R_c=a/2$ (which we refer as main commensurability peak), and $R_c\approx 2.4a$. From the condition $R_c=a/2$, we obtain the Fermi velocity of the electrons that contribute to the resistivity peaks. Figure 2(b) shows the resistivity for the PQW sample with array periodicity $a=0.7$ μm, the commensurability peaks correspond to the conditions $R_c=a/2$ and $R_c\approx 1.9a$. The increment on the resistivity reduces the electron mobility to $\approx 2.3\ 10^3$ cm^2/V s. By comparison with resistivity measurements in the unpatterned region of the samples we can observe that commensurability oscillations do not exist in absence of the cylindrical voids. At the inset, we show the normalized magnetoresitance with respect to the field at $B=0$ T and to

Poly(methyl methacrylate) layer of each bar through high energy electron-beam lithography. The antidot lattice period a was chosen to be 0.6, 0.7, and 0.8 μm for each sample. The antidot pattern was transferred across the AlGaAs parabolic well by plasma etching. The physical diameter of the antidots, d, is approximately 0.1 μm.

Experimental magnetotransport measurements were performed at the temperature of 1.4 K; we employed lock-in technique for detection, with an ac not exceeding 10^{-6} A, the distance between longitudinal potentiometric probes is 100 μm. Longitudinal and transversal resistances were simultaneously recorded for different angles between the magnetic field and the substrate plane, using an *in situ* system for rotation of the samples. $\Theta=90°$ corresponds to perpendicular configuration and $\Theta=0°$ corresponds to the magnetic field parallel to the sample surface. The designed three-dimensional pseudocharge $n^+=n_{3D}$, of the 2000-Å PQW, is $2.1\ 10^{16}$ cm^{-3}, which corresponds to the classical width of the 3DEG slab of $W_e=N_s/n_{3D}=1900$ Å. A direct comparison between longitudinal R_{xx} and transversal resistance R_{xy}, from the patterned and unpatterned regions of the sample, can be done due to the Hall device geometry. The electron mobility μ_e, in the region of the samples without antidots, ranges between $4.3\ 10^4$ cm^2/V s to $5.8\ 10^4$ cm^2/V s, and the
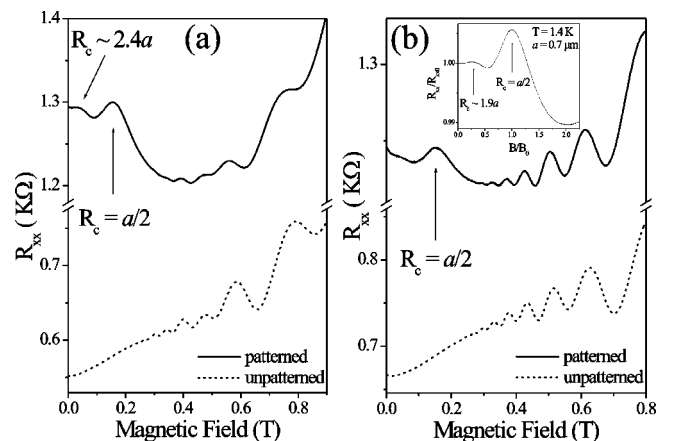

FIG. 2. Experimental magnetoresistance R_{xx} at 1.4 K from the patterned and unpatterned regions of the same PQW sample. (a) The antidot lattice period is $a=0.8$ μm, and (b) The antidot lattice period is $a=0.7$ μm.

the magnetic field that produces a cyclotron diameter that matches the artificial lattice period, we applied a small and additional dc to suppress the weak localization peak around $B = 0$ T. In this way it is possible to observe the exact position of the peaks. Through self-consistent calculations we obtain five occupied subbands for the designed density n_{3D}; in the case of independent two-dimensional subbands it may be possible to expect the observation of several commensurability peaks; however, the strong scattering between the subbands may result in a single main commensurability peak. In order to analyze the influence of the three-dimensional electron gas on the observed structures at low field, we performed magnetoresistance measurements in a tilted magnetic field.

Figure 3(a) shows the magnetoresistance oscillations, at 1.4 K, for different angles Θ, between the field and the substrate plane, for the patterned region of the PQW sample with $a = 0.6$ μm. Figures 3(b) and 3(c) show the three-dimensional representation of the evolution of the commensurability peaks depicted in part (a), seen from the front and back sides, in order to observe all the details of this transformation. In the presence of perpendicular magnetic field, $\Theta = 90°$, we observe two commensurability peaks, the wider corresponds to $R_c = a/2$ and the other to $R_c \approx 1.8a$. According to the position of the peaks there is a correspondence with the measurements in two-dimensional systems with single subband occupation. When the parallel component of the magnetic field is increased, the commensurability peaks are continuously shifted towards the higher values of the field, as it may be expected for two-dimensional antidot systems, in the presence of a tilted magnetic field. However, for certain values of the angle Θ, the peaks deviate from the $[\sin(\Theta)]^{-1}$ dependence and begin to suffer a sudden transformation to a new kind of peaks (also see Fig. 4) that we attributed to size effects due to the commensurability between the cyclotron radius and the well width.[7]

This behavior is opposite to the case of antidots in two-dimensional systems where the shift of the peaks extend continuously to higher values of the magnetic field, this is the main difference between the dynamics of two-dimensional and three-dimensional antidot lattices. This anomalous behavior can be explained with the assumption of a geometrical model, which can help confirm the existence of a 3DEG. Figure 5 on top shows a schematics of a cylindrical void scaled in terms of the artificial lattice period, the dimensions correspond to an antidot with $a = 0.6$ μm on the 2000 Å PQW sample. Physically the two ends of the cylinder are bounded by the interfaces of the well. When the magnetic field is applied perpendicular to the surface of the sample we may assume, disregarding imperfections, that the transversal cross section of the void is exactly a circle. When the whole sample is tilted with respect to the field vector, the transversal cross section of the cylindrical scatterer, which is perpendicular to the field, changes continuously from circular to elliptical up to certain point where the elliptical cross section reaches the diagonal of the void. In this situation the cross section makes an angle $\Theta \approx 27°$ with the magnetic field vector, as shown on the sequence, at bottom of Fig. 5. This construction suggests that the variation of the in-plane sec-
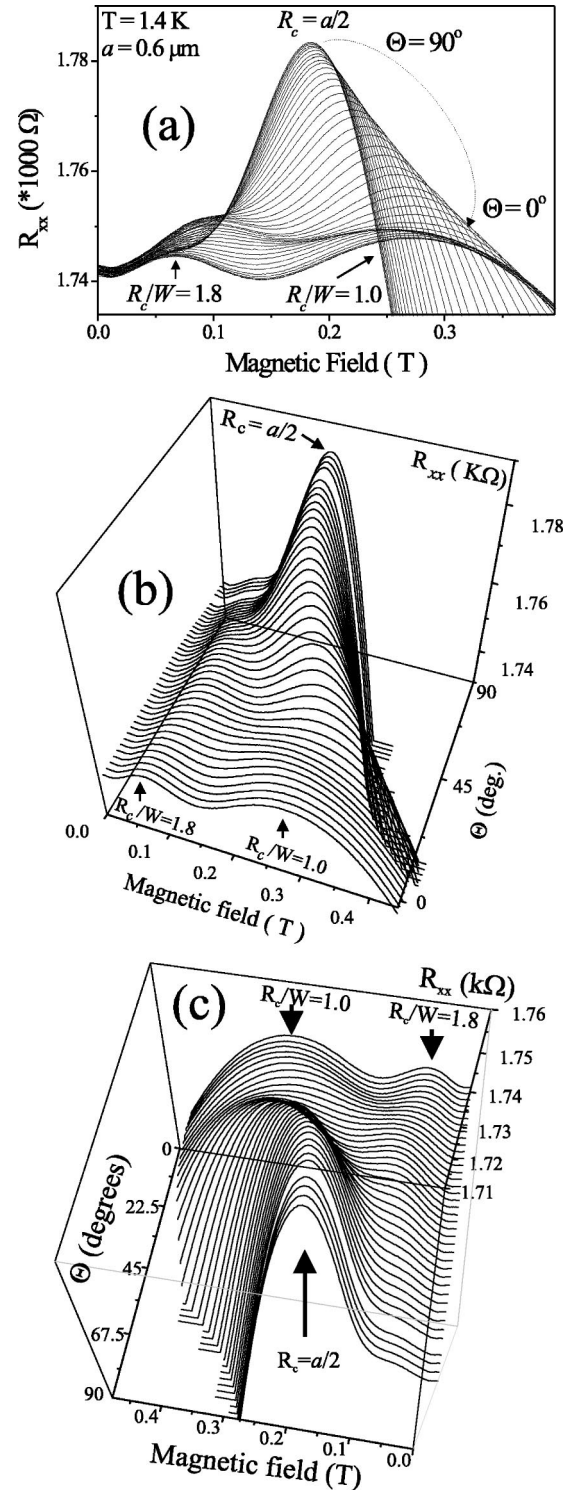

FIG. 3. (a) Magnetoresistance measurements in a tilted magnetic field for the patterned region of the PQW sample with lattice period $a = 0.6$ μ. (b) and (c) Three-dimensional representation of the curves shown in part (a).

tion of the void, from circular to elliptical, must be responsible for the continuous shift of the position of the main commensurability peak only, up to certain values of the angle Θ. From the figure it is possible to infer that when the angle Θ is $\approx 27°$, the regular electron orbits pinned by the void
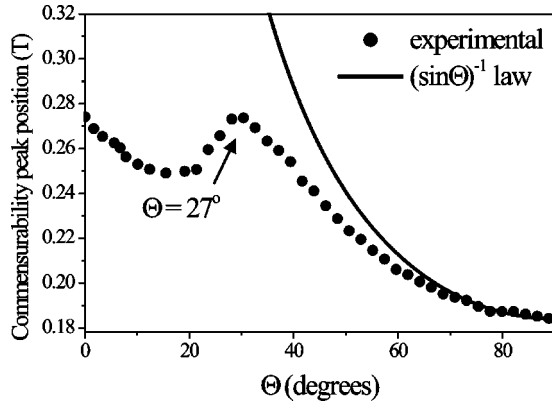
FIG. 4. Shift of the main commensurability peak as a function of angle Θ, between the surface plane and the magnetic field vector. These data were extracted from Fig. 3. The solid line represents the $[\sin(\Theta)]^{-1}$ dependence observed in two-dimensional antidot systems.

cannot be formed anymore and instead the electron dynamics becomes dominated by geometrical resonances between the cyclotron radius and the well width. It is important to note that, in the region between $\Theta = 27°$ and $\Theta = 0°$, the commensurability oscillations between the cyclotron radius and the void cross section are destroyed, while the geometrical resonances between the cyclotron radius and the well width increases continuously, reaching its maximum value when the magnetic field is completely parallel to the plane of the electron gas. The classical electron dynamics in antidot lattices in PQW, under the influence of perpendicular magnetic field, can be obtained from the single particle Hamiltonian: $H = (1/2m^*)(\vec{p} - e\vec{A})^2 + U_{AD}(x,y) + U_w(z)$, where $\vec{p}$ is the momentum vector, $\vec{A} = (-By/2, Bx/2, 0)$ is the symmetric vector potential, e is the electron charge, m^* is the electron effective mass, $U_{AD}(x,y)$ is the antidot potential,[2] and $U_w(z)$ is the confining potential along z direction. The motion in the x-y plane and in z direction can be treated independently, due to a separation of the degrees of freedom. As the electron motion is unbounded on the x-y plane, we observe that the electron dynamics, in the presence of perpendicular magnetic field, retains essentially similar characteristics as the correspondent dynamics in two-dimensional billiard systems. The resulting three-dimensional motion is a combination of a two-dimensional chaotic motion with the completely integrable motion along z direction. Furthermore, the uncoupling of the motion also leads to a chaotic motion in the x-y plane for different energies E_z, where $E_F = E_{x-y} - E_z$, E_F is the Fermi energy, E_{x-y} is the in-plane energy,
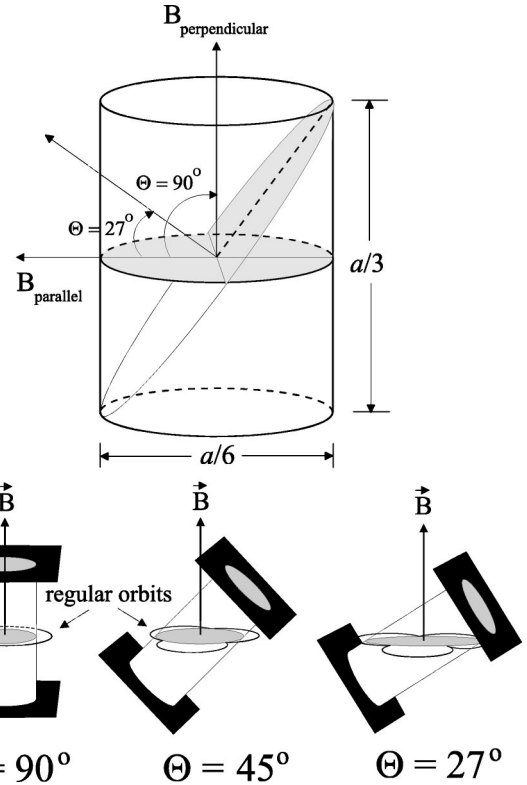

FIG. 5. On top we show the schematics representation of a cylindrical void, with its dimensions scaled in terms of the antidot lattice a, for a 2000-Å PQW sample. At bottom, variation of the shape of the transversal cross section of the void in relation to the direction of the magnetic field vector.

and E_z is the energy along z direction. As $R_c = (1/eB)\sqrt{2m^* E_{x-y}}$, the amplitude of the commensurability peaks get smeared out due to energy averaging; this may be the reason for the broadening of the peaks, which was observed in the experiments. In summary, the achievement of a three-dimensional electron billiard system has been accomplished in this work, through the patterning of arrays of cylindrical voids, on $Al_xGa_{1-x}As/GaAs$ PQW semiconductor heterostructures. This construction can be introduced as a tool to extend the study of chaotic electron dynamics, in condensed matter physics, to the systems with a higher dimensionality.

---

*Also at INSA-Toulouse, 31077, Cedex 4, France and Institut Universitaire de France, Toulouse, France.

[1] D. Weiss, M.L. Roukes, A. Menschig, P. Grambow, K. von Klitzing, and G. Weimann, Phys. Rev. Lett. **66**, 2790 (1991).

[2] R. Fleischmann, T. Geisel, and R. Ketzmerick, Phys. Rev. Lett. **68**, 1367 (1992).

[3] T. Papenbrock, Phys. Rev. E **61**, 4626 (2000).

[4] H. Primack and U. Smilansky, Phys. Rep. **327**, 1 (2000).

[5] V. Celli and N.D. Mermin, Phys. Rev. **140**, A839 (1965).

[6] M. Sundaram, A.C. Gossard, J.H. English, and R.M. Westervelt, Superlattices Microstruct. **4**, 683 (1988).

[7] D.K. Mac Donald, and K. Sarginson, Proc. Roy. Soc. **203A**, 223 (1950).